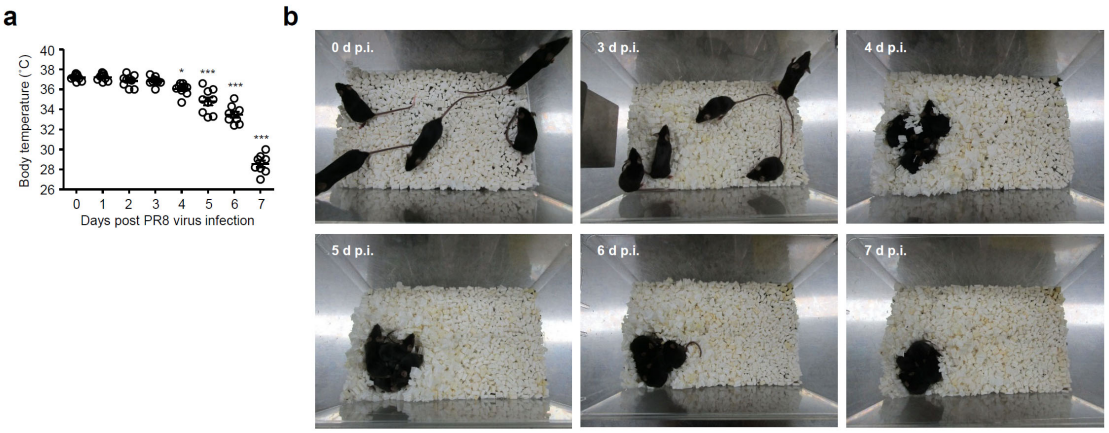

Extended Data Figure 1

Changes of body temperature following influenza virus infection.

a, b, Mice kept at 22 °C were infected intranasally with 1,000 pfu of influenza virus. Core body temperatures (**a**) and activity of infected mice (**b**) were monitored for 7 days.

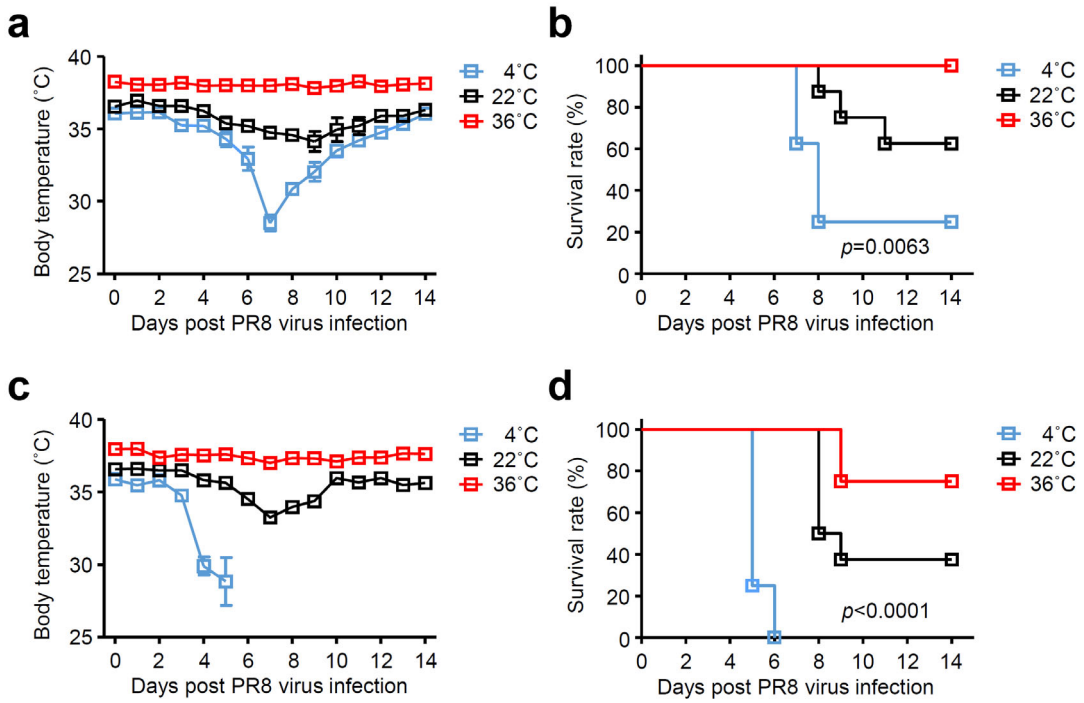

Extended Data Figure 2

Core body temperature affects severity of influenza virus infection.

a-d, Mice were kept at 4, 22, or 36 °C for 7 d before influenza virus infection and throughout infection. Mice kept at 4, 22, or 36 °C were infected intranasally with 500 (**a, b**) or 2,000 (**c, d**) pfu of influenza virus. Core body temperatures (**a, c**) and mortality (**b, d**) were monitored for 14 days.

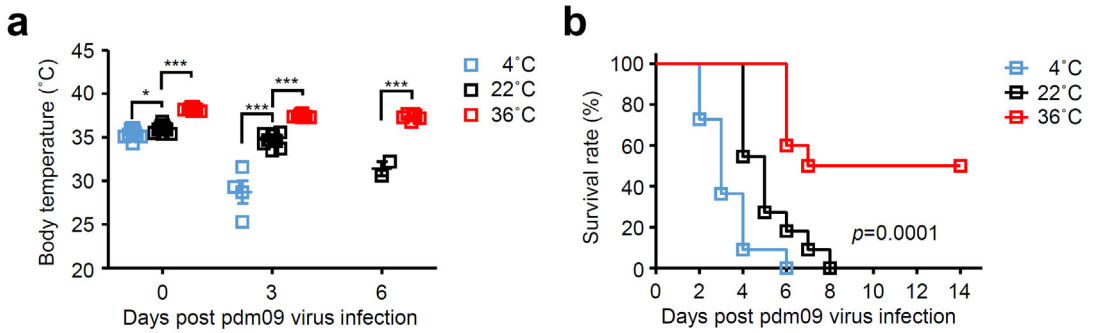

Extended Data Figure 3

Core body temperature affects severity of influenza virus pdm09 infection.

a, b, Mice were kept at 4, 22, or 36 °C for 7 d before influenza virus infection and throughout infection. Mice kept at 4, 22, or 36 °C were infected intranasally with 3×10^4 pfu of a human isolate of the 2009 pandemic influenza A virus strain A/Narita/1/2009 (pdm09). Core body temperatures (**a**) and mortality (**b**) were monitored for 14 days.

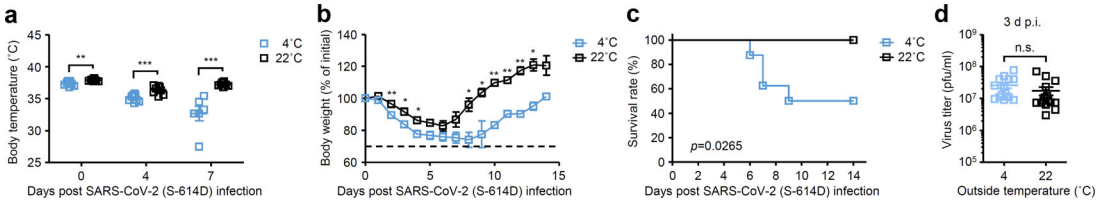

Extended Data Figure 4

Effects of outside temperature on severity of SARS-CoV-2 infection.

a-d, Syrian hamsters were kept at 4 or 22 °C for 7 d before original SARS-CoV-2 (S-614D) infection and throughout infection. Hamsters kept at 4 or 22 °C were infected intranasally with 1.5×10^6 pfu of an original SARS-CoV-2 (S-614D) strain. Core body temperatures (**a**), wight loss (**b**), mortality (**c**), and virus titer in the lung wash (**d**) were measured on indicated days after challenge. The dashed line indicates the limit of endpoint.

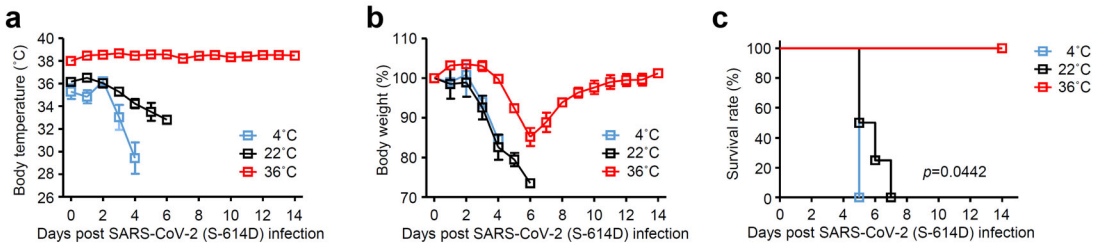

Extended Data Figure 5

Core body temperature affects severity of SARS-CoV-2 infection.

a-c, K18-hACE2 mice were kept at 4, 22, or 36 °C for 7 d before original SARS-CoV-2 (S-614D) infection and throughout infection. K18-hACE2 mice kept at 4, 22, or 36 °C were infected intranasally with 5×10^4 pfu of an original SARS-CoV-2 (S-614D) strain. Core body temperatures (**a**), weight loss (**b**), and mortality (**c**) were monitored for 14 days.

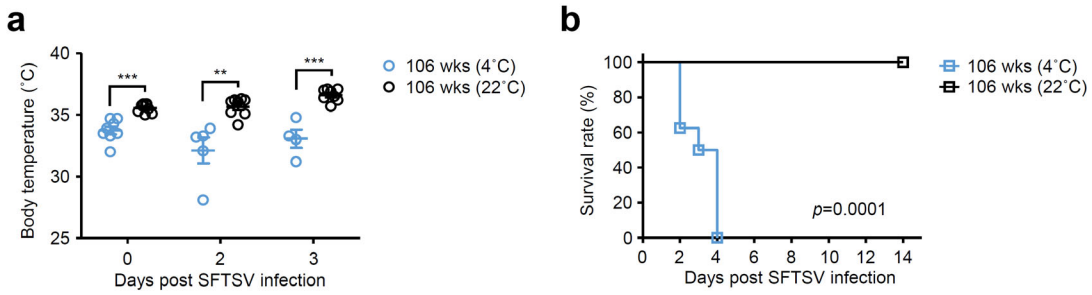

Extended Data Figure 6

Effects of outside temperature on severity of SFTSV infection.

a, b, One hundred six-weeks-old mice were kept at 4 or 22 °C for 7 d before SFTSV infection and throughout infection. 106-weeks-old mice kept at 4 or 22°C were infected intravenously with 5×10^6 $TCID_{50}$ of SFTSV. Core body temperatures (**a**) and mortality (**b**) were measured on indicated days after challenge.

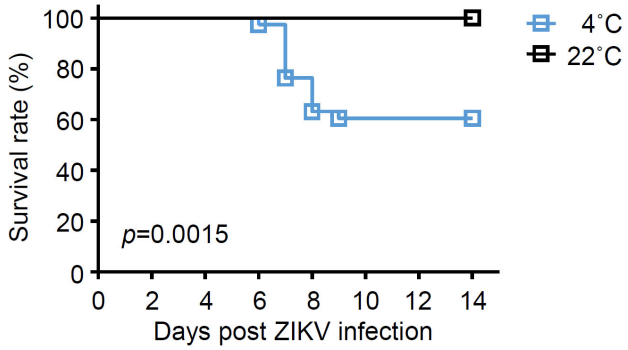

Extended Data Figure 7

Effects of outside temperature on severity of ZIKV infection.

Mice were kept at 4 or 22 °C for 7 d before ZIKV infection and throughout infection. Mice kept at 4 or 22°C were infected intravenously with 1.5×10^7 pfu of ZIKV. Mortality was monitored for 14 days.

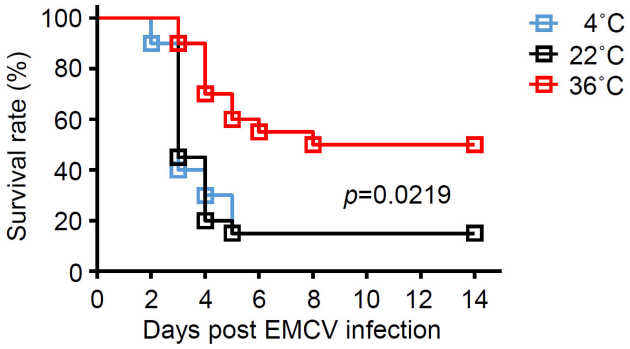

Supplementary Data Figure 8

Effects of outside temperature on severity of EMCV infection.

Mice were kept at 4, 22, or 36 °C for 7 d before EMCV infection and throughout infection. Mice kept at 4, 22, or 36 °C were infected intraperitoneally with 100 pfu of EMCV. Mortality was monitored for 14 days.

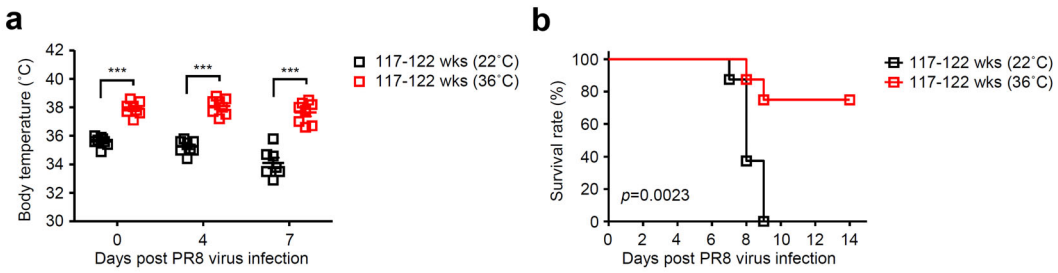

Extended Data Figure 9

High-heat exposure of aged mice had improved survival after influenza virus infection.

a, b, One hundred seventeen- to 122-weeks-old mice were kept at 22 or 36 °C for 7 d before influenza virus infection and throughout infection. Mice kept at 22 or 36°C were infected intranasally with 1,000 pfu of influenza virus. Core body temperatures (**a**) and mortality (**b**) were measured on indicated days after challenge.

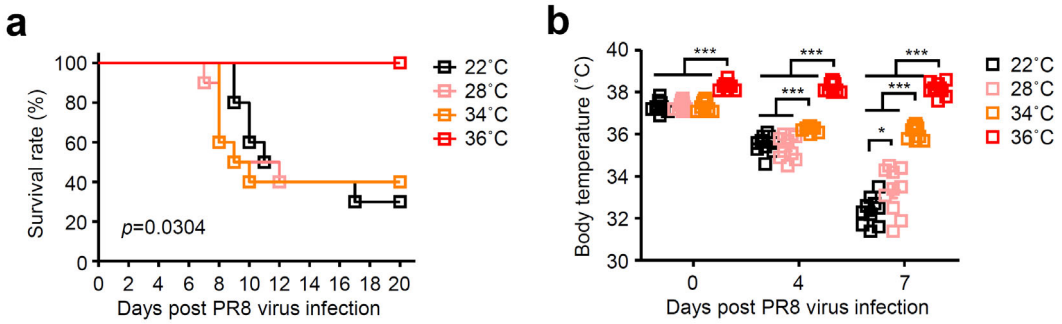

Extended Data Figure 10

Effects of outside temperature on severity of influenza virus infection.

a, b, Mice were kept at 22, 28, 34, or 36 °C for 7 d before influenza virus infection and throughout infection. Mice kept at 22, 28, 34, or 36 °C were infected intranasally with influenza virus. Mortality (**a**) and core body temperatures (**b**) were measured on indicated days after challenge.

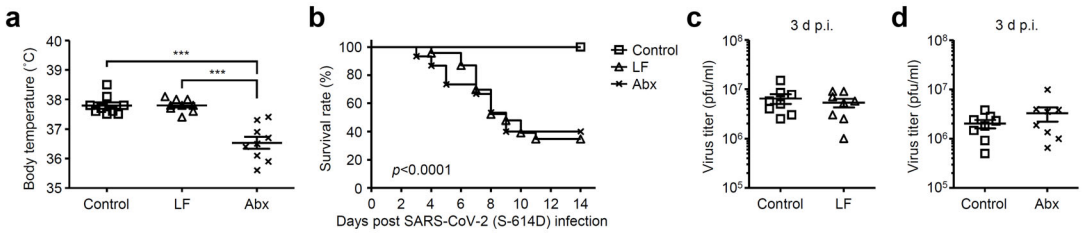

Extended Data Figure 11

Gut microbiota-derived metabolites protect hamsters from SARS-CoV-2 infection.

a-d, Six-weeks-old hamsters were fed a low fiber (LF)-diet (AIN93G) or antibiotics (Abx) in drinking water for 2 weeks before SARS-CoV-2 infection. Core body temperature of LF-fed, Abx-treated, and control uninfected hamsters kept at 22 °C were measured (**a**). LF-fed, Abx-treated, and control hamsters kept at 22 °C were infected intranasally with 1.5×10^6 pfu of an original SARS-CoV-2 (S-614D) strain. Mortality (**b**) and virus titer in the lung wash (**c, d**) were measured on indicated days after challenge.

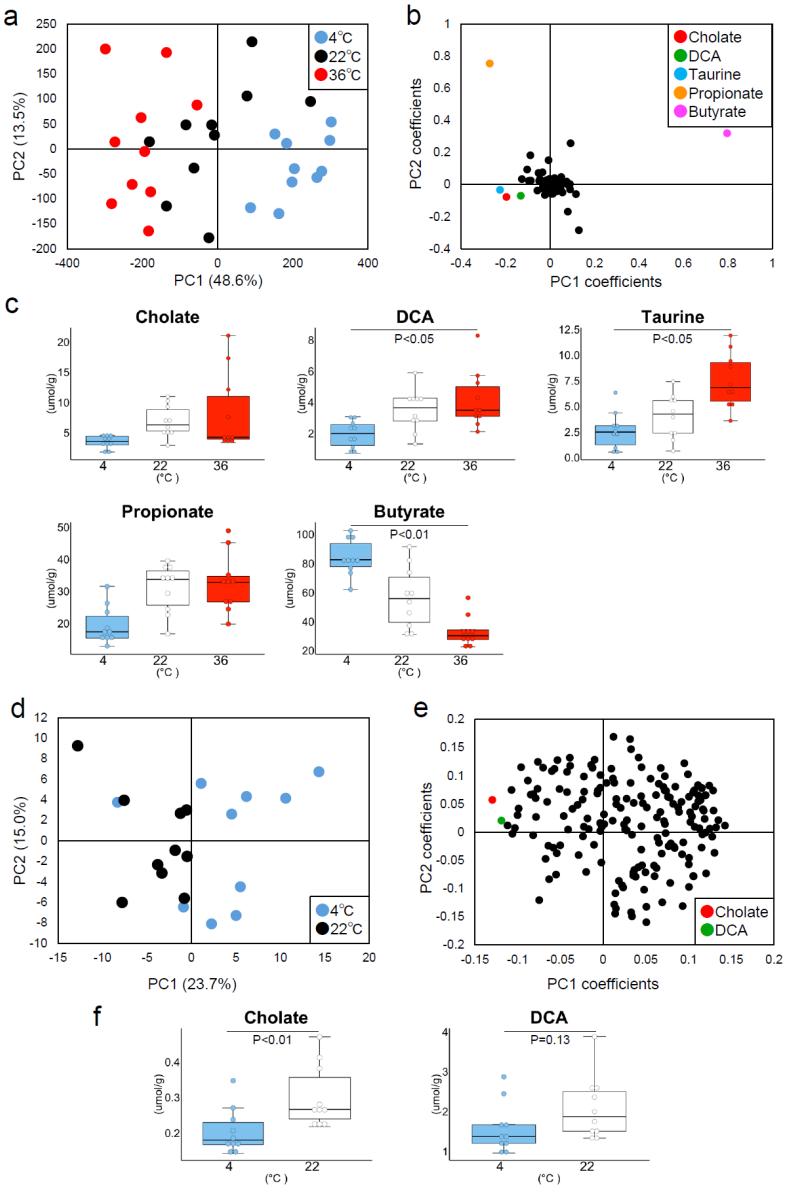

Extended Data Figure 12

Effects of outside temperature on the cecal metabolome profiles of mice and hamsters.

a, b, PCA plot of the cecal metabolome profiles in mice normalized by Pareto (**a**) and loading scatter plot (**b**). **c,** Box plots indicating cecal amounts of metabolites in mice that had |PC1 coefficient values| > 0.13 in PCA. Significant differences are indicated based on Tukey–Kramer test. **d, e,** PCA plot of the cecal metabolome profiles in Syrian hamster normalized by unit variance (**d**) and loading scatter plot (**e**). **f,** Box plots indicating cecal amounts of metabolites in Syrian hamster that had PC1 coefficient values < -0.115 in PCA. Significant differences are indicated based on Student's t-test.

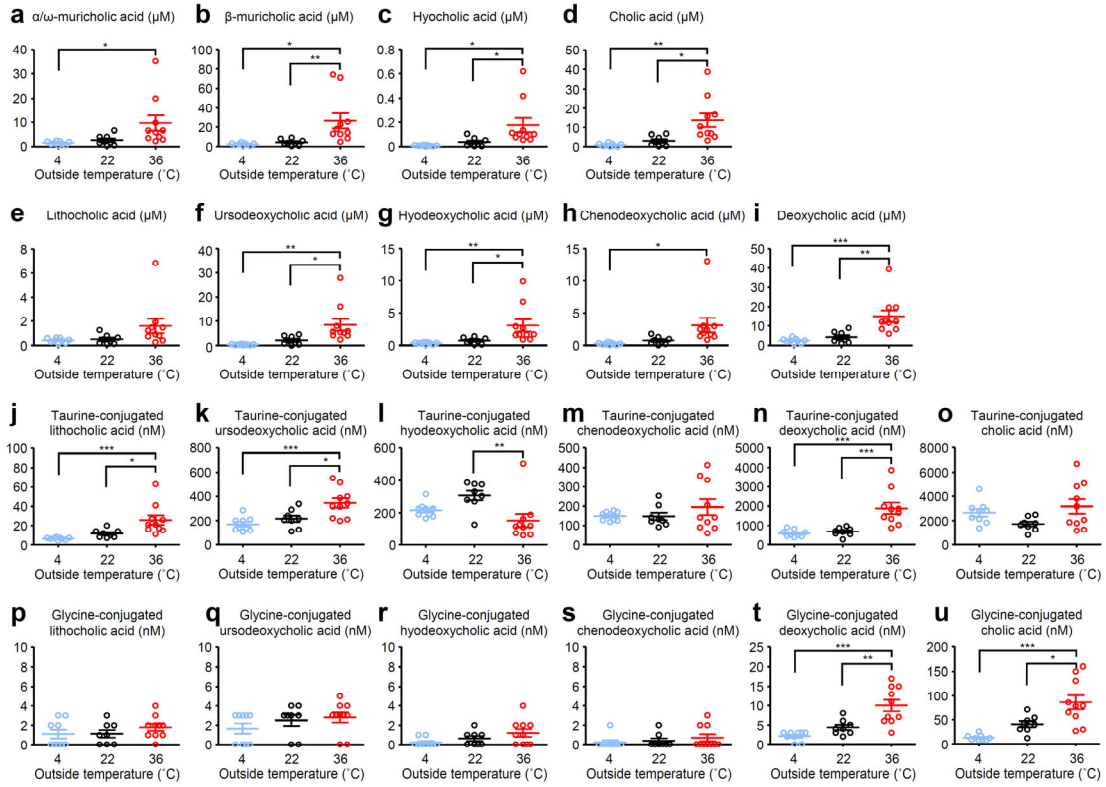

Extended Data Figure 13

The levels of bile acids in serum.

a-u, Mice were kept at 4, 22, or 36 °C for 7 d. The levels of bile acids in cecal contents were measured.

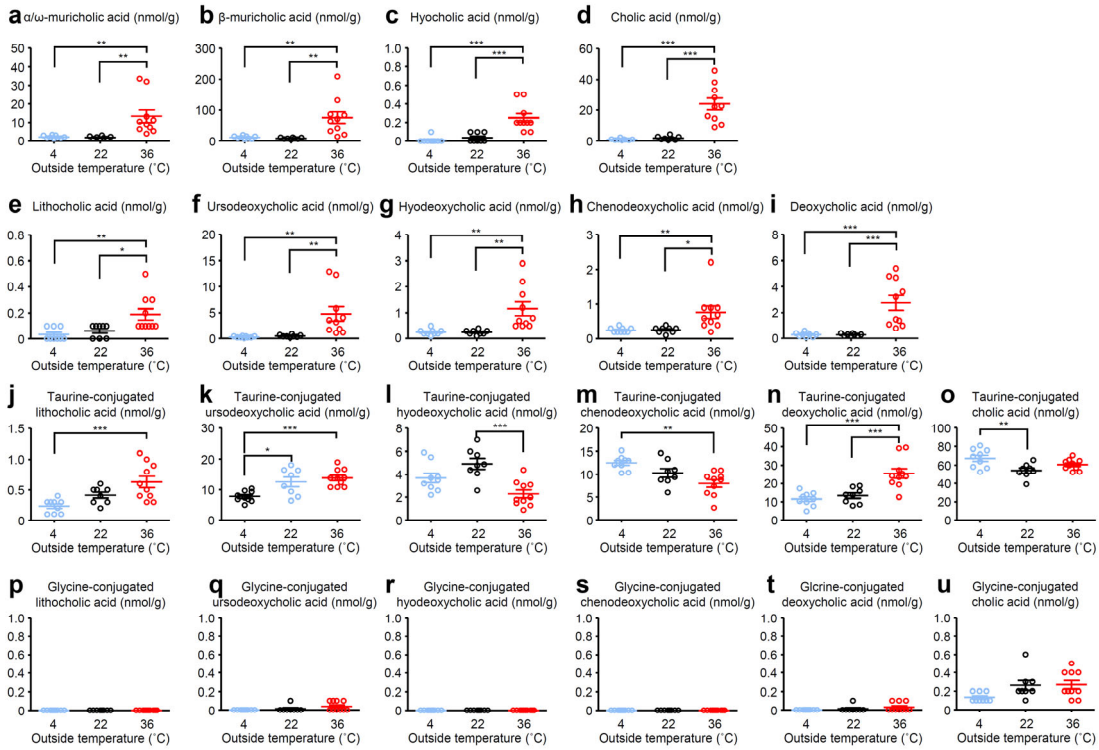

Extended Data Figure 14

The levels of bile acids in Liver.

a-u, Mice were kept at 4, 22, or 36 °C for 7 d. The levels of bile acids in serum were measured.

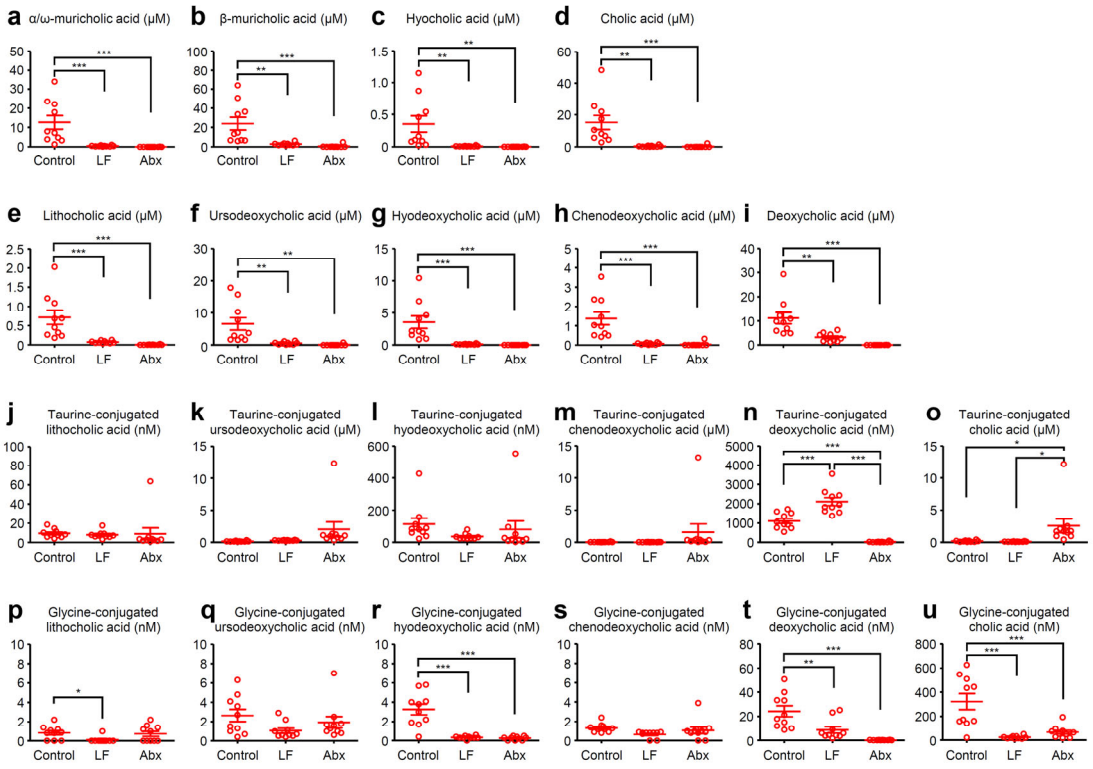

Extended Data Figure 15

The levels of bile acids in serum of high heat-exposed mice.

a-u, LF-fed, Abx-treated, and control mice were kept at 36 °C for 7 d. The levels of bile acids in serum were measured.

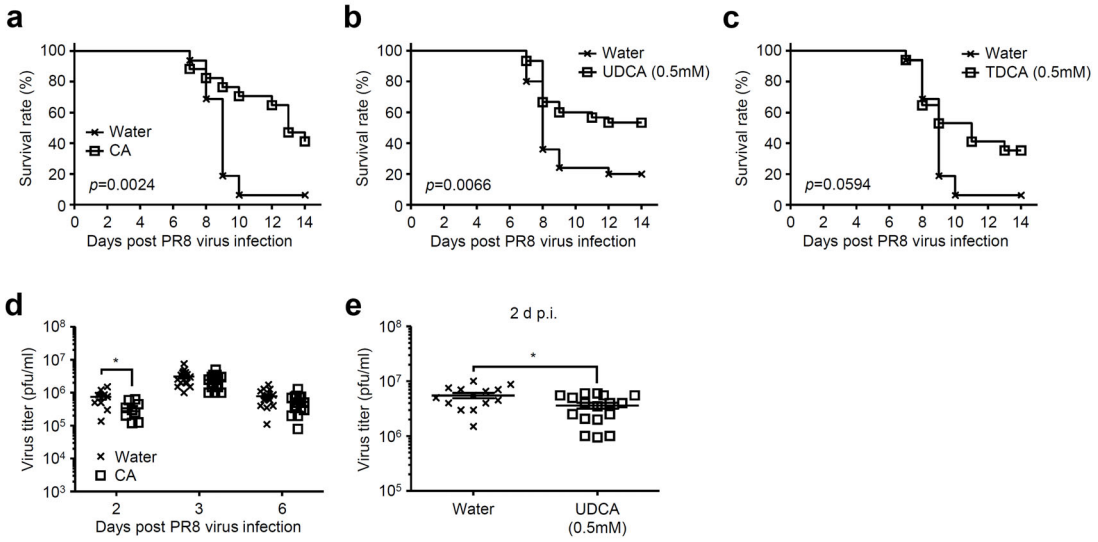

Extended Data Figure 16

Bile acids protect mice from influenza virus infection.

a-e, CA- (**a, d**), UDCA- (**b, e**) or TDCA-treated (**c**) mice kept at 22 °C were infected intranasally with 1,000 pfu of influenza virus. Mortality (**a-c**) and virus titer in the lung wash (**d, e**) were measured on indicated days after challenge.

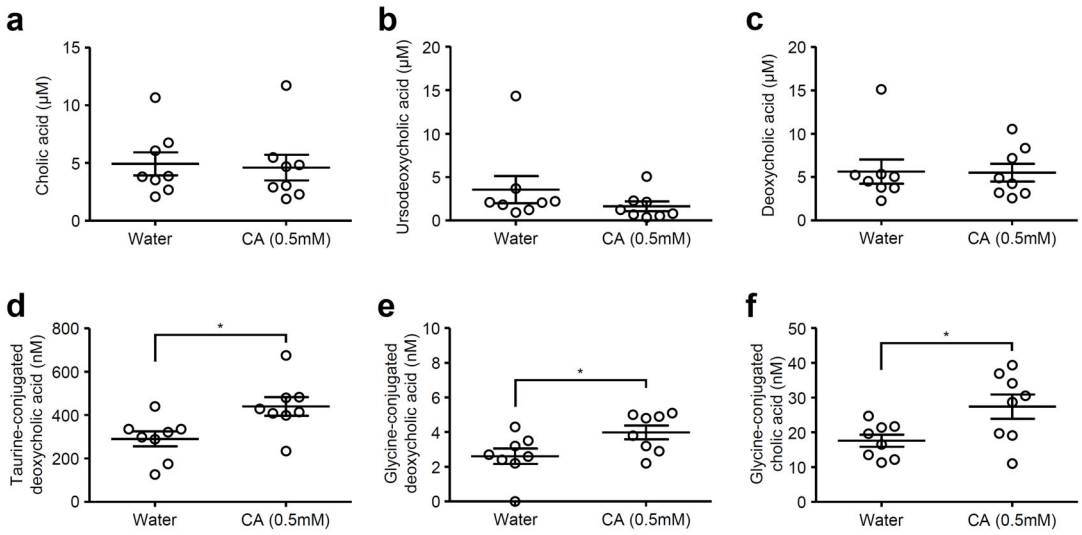

Extended Data Figure 17

The levels of bile acids in serum of control or CA-treated mice.

a-f, CA-treated or control mice were kept at 22°C for 7 d. The levels of bile acids in serum were measured.

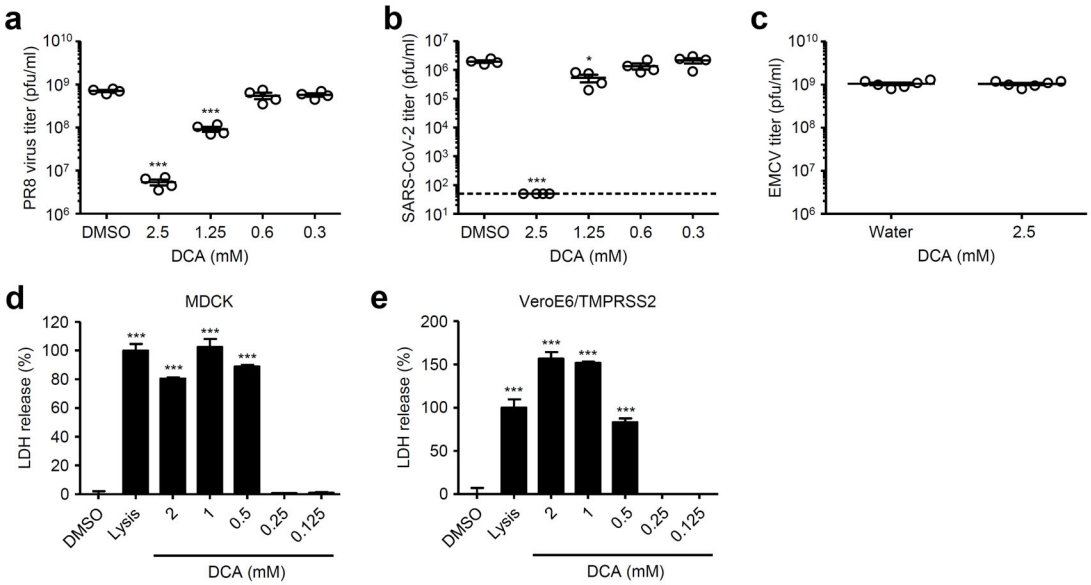

Extended Data Figure 18

Bile acids directly disrupt enveloped viruses.

a-c, Influenza virus (**a**), SARS-CoV-2 (**b**), and EMCV (**c**) were incubated with indicated amounts of DCA at 37 °C for 1 h. Virus titers were measured by standard plaque assay using MDCK (**a**), VeroE6/TMPRSS2 (**b**), or L929 cells (**c**). **d, e,** Uninfected-MDCK (**d**) or VeroE6/TMPRSS2 (**e**) cells were cultured in the presence or absence of indicated amounts of DCA for 24 h. LDH activity was measured for cytotoxicity.

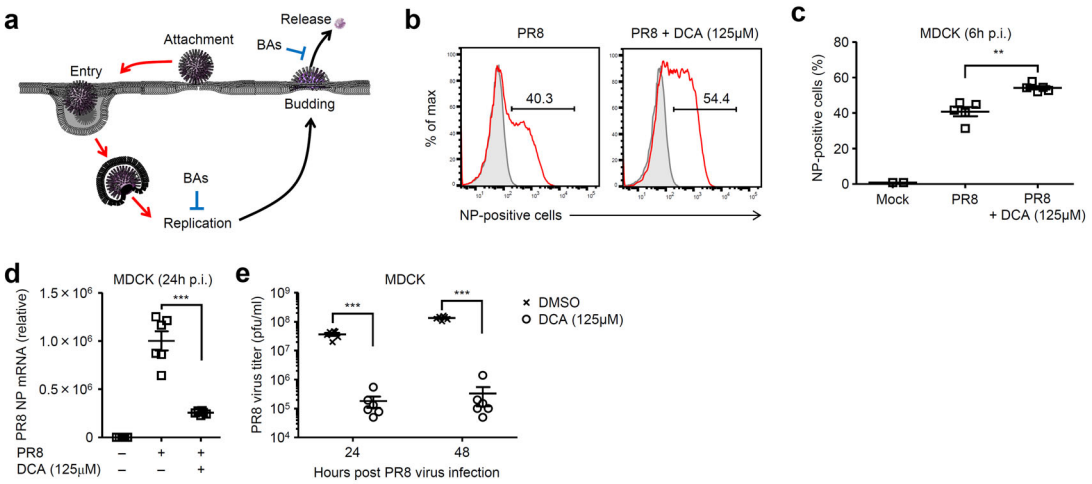

Extended Data Figure 19

Bile acids inhibit influenza virus replication.

a, Effects of bile acids (BAs) on influenza virus replication. Red arrows indicate enhancement. Blue blunt ended bars indicate inhibition. **b-e,** MDCK cells were infected with influenza virus in the presence or absence of 125 μM of DCA. Cells were collected at 6 h post infection, and intracellularly stained with nucleoprotein (NP)-specific antibody (**b**). Percentages of NP-positive cells are shown (**c**). Total RNAs were extracted from uninfected or virus-infected cells at 24 h p.i. and influenza virus NP mRNA levels were assessed by quantitative reverse transcription PCR (**d**). Cell-free supernatants were collected at 24 and 48 h p.i. and analyzed for virus titer by standard plaque assay using MDCK cells (**e**).

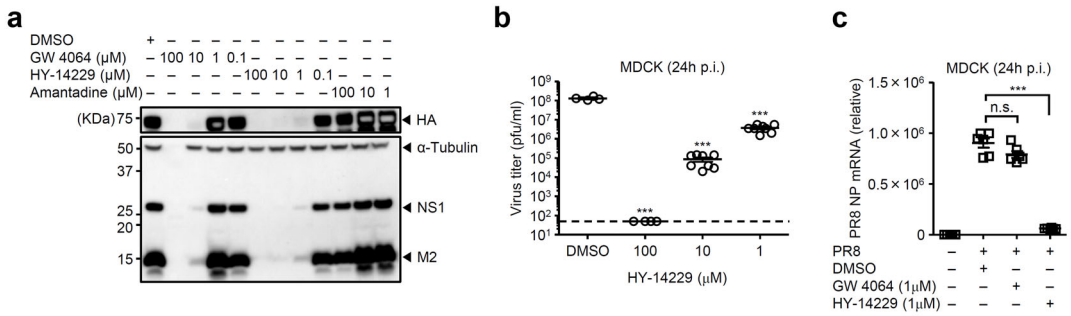

Extended Data Figure 20

Effects of TGR5 and FXR agonists on influenza virus replication.

a-c, MDCK cells were infected with influenza virus PR8 (an amantadine-resistant strain) in the presence or absence of indicated amounts of GW 4064, HY-14229, or amantadine. Cell lysates were collected at 24 h p.i. and analyzed by immunoblotting with indicated antibodies (**a**). Cell-free supernatants were collected at 24 h p.i. and analyzed for virus titer by standard plaque assay using MDCK cells (**b**). Total RNAs were extracted from uninfected or virus-infected cells at 24 h p.i. and influenza virus NP mRNA levels were assessed by quantitative reverse transcription PCR (**c**).

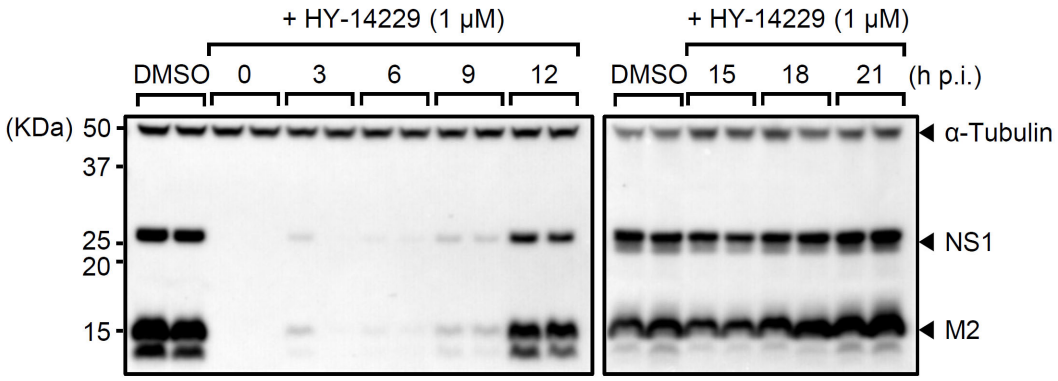

Extended Data Figure 21

Therapeutic effects of HY-14229 on influenza virus replication.

MDCK cells were infected with influenza virus PR8. After infection, the culture medium was replaced with medium with 1 μM of HY-14229 at indicated time points. Cell lysates were collected at 24 h p.i. and analyzed by immunoblotting with indicated antibodies.

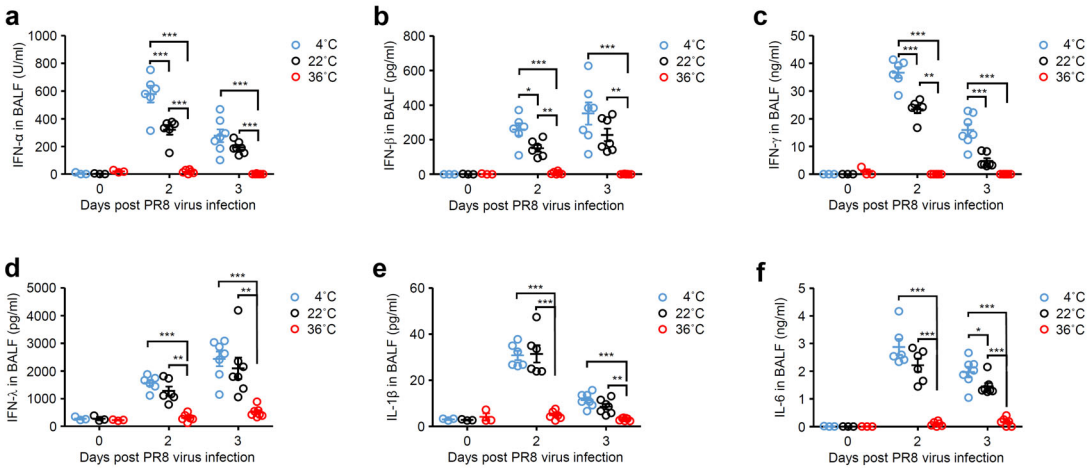

Extended Data Figure 22

Effects of outside temperature on influenza virus-induced cytokine production.

a-f, Mice were kept at 4, 22, or 36 °C for 7 d before influenza virus infection and throughout infection. Mice kept at 4, 22, or 36 °C were infected intranasally with 1,000 pfu of influenza virus. The lung washes were collected at indicated time points and analyzed for IFN-α (**a**), IFN-β (**b**), IFN-γ (**c**), IFN-λ (**d**), IL-1β (**e**), and IL-6 (**f**).

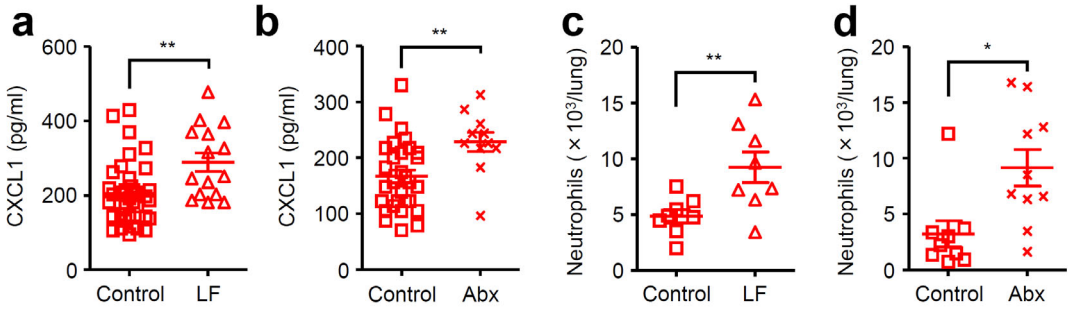

Extended Data Figure 23

Effects of outside temperature on influenza virus-induced cytokine production.

a-d, LF-fed, Abx-treated, and control mice kept at 36 °C were infected intranasally with 1,000 pfu of influenza virus. The lung washes were collected at 4 d p.i. and analyzed for CXCL1 by ELISA (**a, b**). Lymphocytes were isolated from the lung at 7 d p.i.. The number of $Ly6C^+$ $Ly6G^+$ neutrophils were analyzed by flow cytometry (c, d).

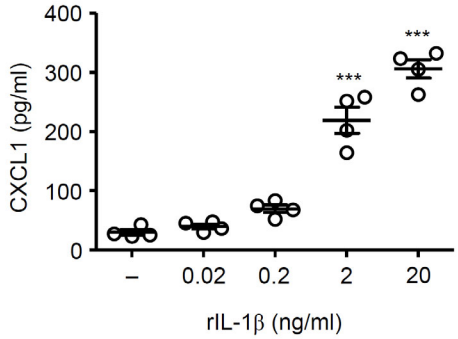

Extended Data Figure 24

Treatment of BMMs with IL-1β stimulates CXCL1 production.

BMMs were stimulated with indicated amounts of recombinant mouse IL-1β (rIL-1β). Cell-free supernatants were collected at 24 h post stimulation and analyzed for CXCL1 by ELISA.

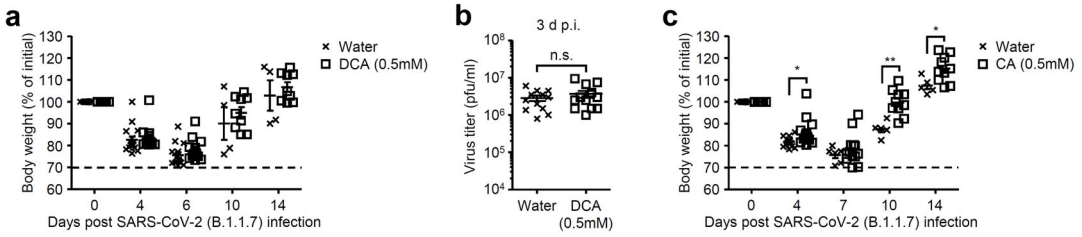

Extended Data Figure 25

Weight loss and virus titer of SARS-CoV-2-infected hamsters.

a-c, DCA- (**a, b**) or CA-treated (**c**) hamsters kept at 22°C were infected intranasally with 1.5×10^6 pfu of SARS-CoV-2 B.1.1.7 (alpha) variant. Weight loss (**a, c**) and virus titer in the lung wash (**b**) were measured on indicated days after challenge. The dashed line indicates the limit of endpoint.

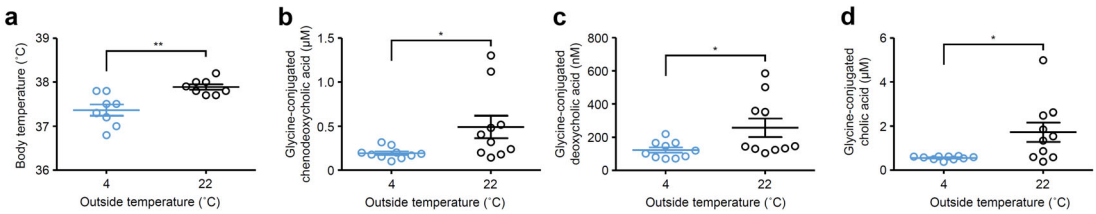

Extended Data Figure 26

Body temperature and the levels of bile acids in serum of cold- and RT-exposed hamsters.

a-d, Hamsters were kept at 4 or 22 °C for 7 d. Core body temperature (**a**) and the levels of bile acids in serum (**b**) of naïve hamsters were measured.

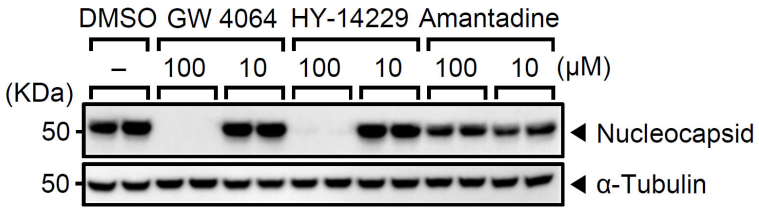

Extended Data Figure 27

Effects of TGR5 and FXR agonists on SARS-CoV-2 replication.

VeroE6/TMPRSS2 cells were infected with original SARS-CoV-2 (S-614D) in the presence or absence of indicated amounts of GW 4064, HY-14229, or amantadine. Cell lysates were collected at 24 h p.i. and analyzed by immunoblotting with indicated antibodies.

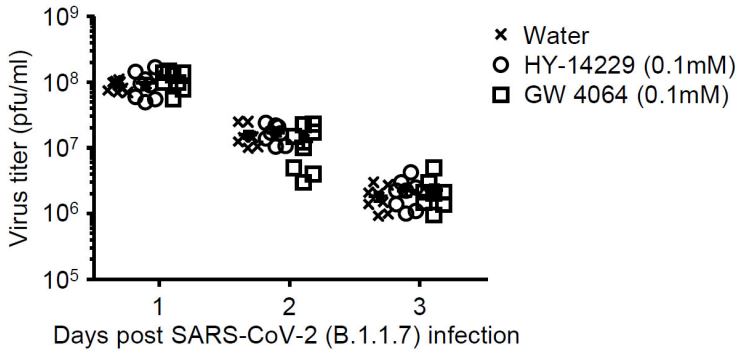

Extended Data Figure 28

Effects of TGR5 and FXR agonists on SARS-CoV-2 replication in hamsters.

HY-14229-, GW 4064-treated or control hamsters kept at 22°C were infected intranasally with 1.5×10^6 pfu of SARS-CoV-2 B.1.1.7 (alpha) variant. Virus titers in the lung washes were measured on indicated days after challenge.

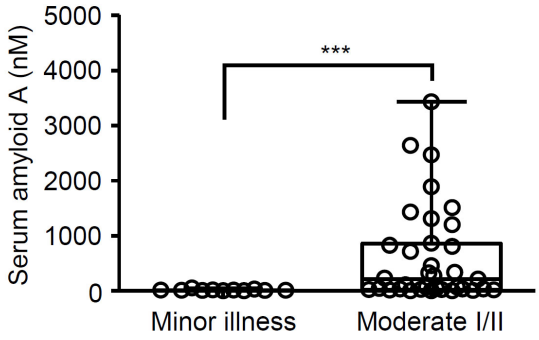

Extended Data Figure 29

Level of serum amyloid A in plasma of COVID-19 patients.

Concentrations of serum amyloid A in plasma of minor (n = 11) versus moderate I/II (n = 35) groups were measured. Each dot represents a unique patient.

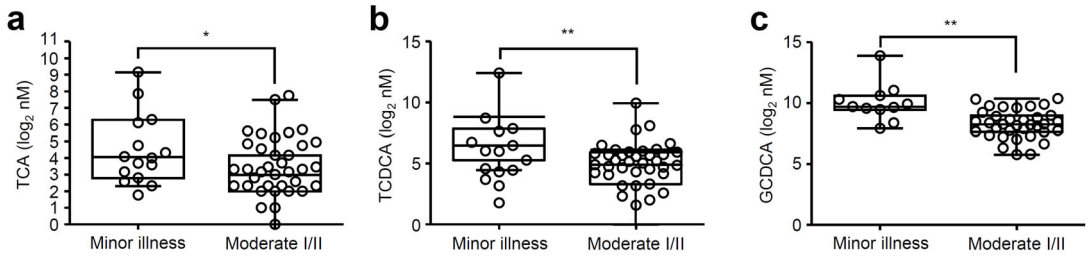

Extended Data Figure 30

Levels of bile acids in plasma of COVID-19 patients.

a-c, Concentrations of taurine-conjugated CA (TCA) (**a**), taurine-conjugated chenodeoxycholic acid (TCDCA) (**b**), and glycine-conjugated chenodeoxycholic acid (GCDCA) (**c**) in plasma of minor (n = 11) versus moderate I/II (n = 35) groups were measured. Each dot represents a unique patient.

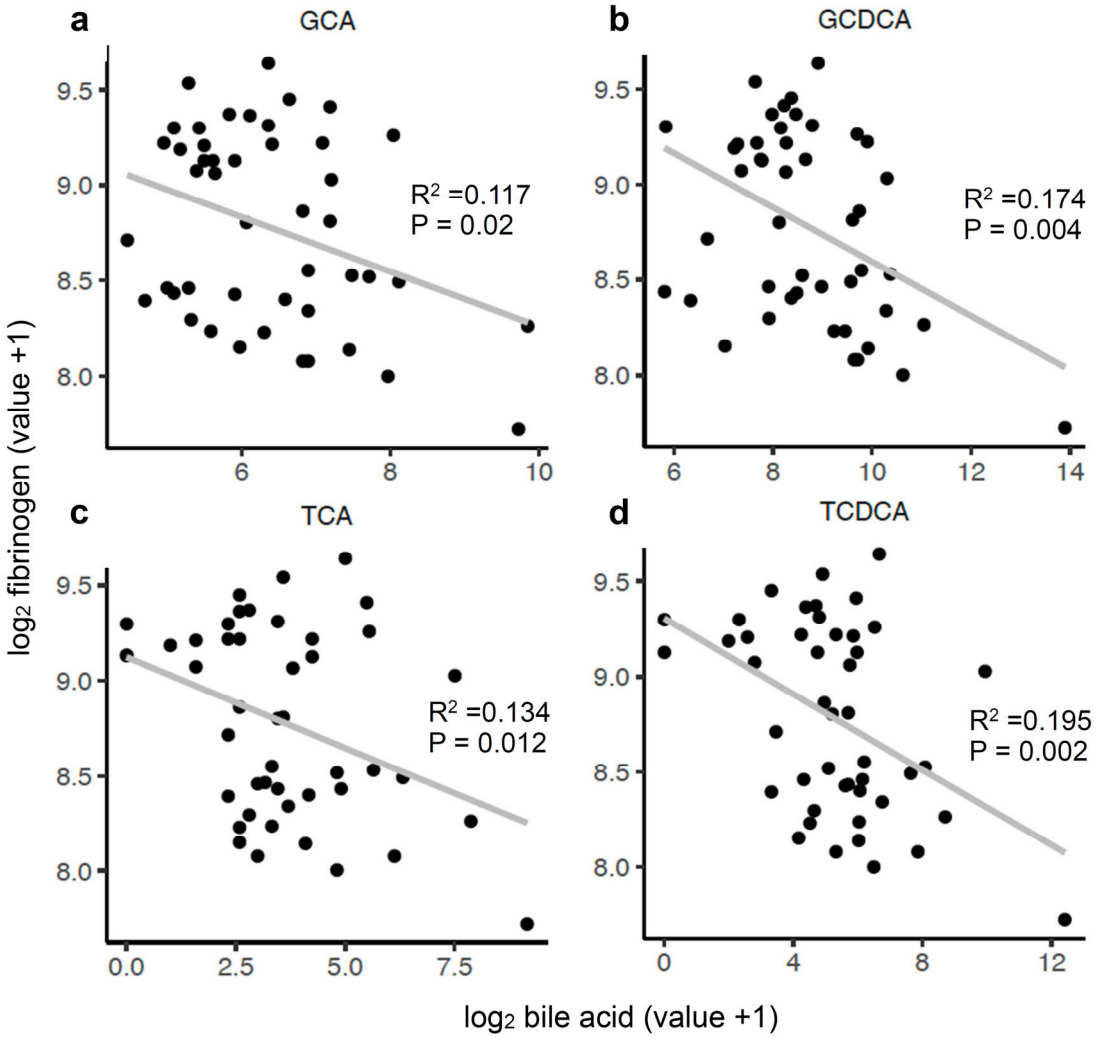

Extended Data Figure 31

The levels of plasma bile acids in COVID-19 patients were negatively correlated with the level of plasma fibrinogen as a biomarker of COVID-19 disease severity. **a-d,** Scatterplots of the levels of plasma bile acids and a fibrinogen. Individual patients are represented as black circles. The solid gray line shows the regression line. R2 and P values were calculated based on the linear regression and the Wald test, respectively. GCA: glycine-conjugated cholic acid, GCDCA: glycine-conjugated chenodeoxycholic acid, TCA: taurine-conjugated cholic acid, TCDCA: taurine-conjugated chenodeoxycholic acid.

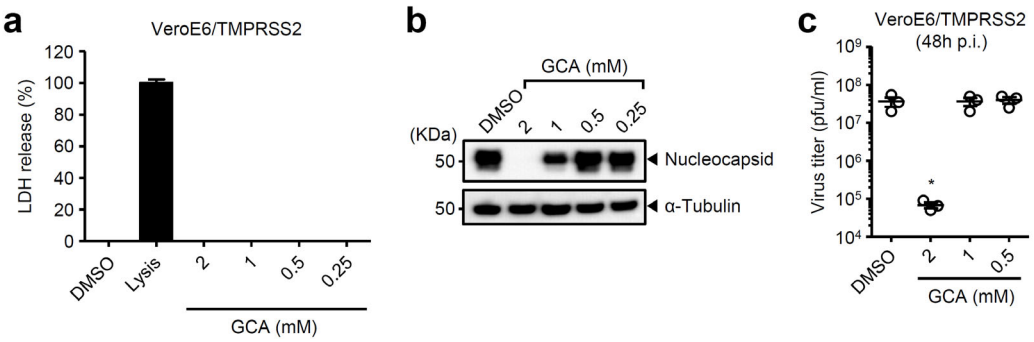

Extended Data Figure 32

GCA inhibits SARS-CoV-2 replication.

a, Uninfected-VeroE6/TMPRSS2 cells were cultured in the presence or absence of indicated amounts of GCA for 24 h. LDH activity was measured for cytotoxicity. **b, c**, VeroE6/TMPRSS2 cells were infected with original SARS-CoV-2 (S-614D) in the presence or absence of indicated amounts of GCA. Cell lysates were collected at 24 h p.i. and analyzed by immunoblotting with indicated antibodies (**b**). Cell-free supernatants were collected at 48 h p.i. and analyzed for virus titer by standard plaque assay using VeroE6/TMPRSS2 cells (**c**).